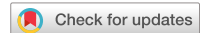


# scientific data



OPEN

DATA DESCRIPTOR

## Comprehensive microRNA-seq transcriptomic profiling across 11 organs, 4 ages, and 2 sexes of Fischer 344 rats

Xintong Yao<sup>1,3</sup>, Shanyue Sun<sup>1,3</sup>, Yi Zi<sup>1</sup>, Yaqing Liu<sup>1</sup>, Jingcheng Yang<sup>1</sup>, Luyao Ren<sup>1</sup>, Guangchun Chen<sup>2</sup>, Zehui Cao<sup>1</sup>, Wanwan Hou<sup>1</sup>, Yueqiang Song<sup>1</sup>, Jun Shang<sup>1</sup>, He Jiang<sup>1</sup>, Zhihui Li<sup>1</sup>, Haiyan Wang<sup>1</sup>, Peipei Zhang<sup>1</sup>, Leming Shi<sup>1</sup>, Quan-Zhen Li<sup>2</sup>✉, Ying Yu<sup>1</sup>✉ & Yuanting Zheng<sup>1</sup>✉

Rat is one of the most widely-used models in chemical safety evaluation and biomedical research. However, the knowledge about its microRNA (miRNA) expression patterns across multiple organs and various developmental stages is still limited. Here, we constructed a comprehensive rat miRNA expression BodyMap using a diverse collection of 320 RNA samples from 11 organs of both sexes of juvenile, adolescent, adult and aged Fischer 344 rats with four biological replicates per group. Following the Illumina TruSeq Small RNA protocol, an average of 5.1 million 50 bp single-end reads was generated per sample, yielding a total of 1.6 billion reads. The quality of the resulting miRNA-seq data was deemed to be high from raw sequences, mapped sequences, and biological reproducibility. Importantly, aliquots of the same RNA samples have previously been used to construct the mRNA BodyMap. The currently presented miRNA-seq dataset along with the existing mRNA-seq dataset from the same RNA samples provides a unique resource for studying the expression characteristics of existing and novel miRNAs, and for integrative analysis of miRNA-mRNA interactions, thereby facilitating better utilization of rats for biomarker discovery.

### Background & Summary

MicroRNAs (miRNAs) are small noncoding RNAs (21–24 nucleotides) that mediate post-transcriptional regulation of gene expression by binding to the 3' untranslated regions of messenger RNAs (mRNA)<sup>1–5</sup>. miRNAs play pivotal roles in biological processes such as differentiation, development, tissue growth, and tumor initiation and progression<sup>2,4,6</sup>. miRNAs can serve as potential clinical biomarkers for disease diagnosis, prognosis, and treatment selection<sup>7–9</sup>, as well as therapeutic targets for human diseases<sup>10–12</sup>. However, the development of miRNA-based biomarkers and therapies is hampered due to incomplete understanding of the characteristics of miRNA profiles across different organs, various developmental stages, or sexes of rat, an extensively used animal model for evaluating drug safety and understanding drug mechanisms of action. Furthermore, the rat miRNA transcriptome is much less well annotated compared to that of mouse and human, with 764, 1915, and 2588 miRNAs annotated in miRBase v.22.1 (<http://www.mirbase.org/>) for rat, mouse, and human, respectively<sup>13,14</sup>. Therefore, characterizing rat miRNA expression profiles more comprehensively is warranted, especially with the advancement of high-throughput technologies such as microarrays and next-generation sequencing.

Several efforts for constructing a catalog of rat miRNA expression have been reported. For example, Minami *et al.*<sup>15</sup> reported a dataset of microarray-based expression profiles of 424 miRNAs cross 55 different organs and tissues of 10-week-old male Sprague-Dawley rats. Similarly, Bushel *et al.*<sup>16</sup> developed the RATEmiRs

<sup>1</sup>State Key Laboratory of Genetic Engineering, Human Genome Institute, School of Life Sciences and Shanghai Cancer Center, Fudan University, Shanghai, 200438, China. <sup>2</sup>Department of Immunology, Microarray and Immune Phenotyping Core Facility, University of Texas Southwestern Medical Center, Dallas, TX, 75390, USA. <sup>3</sup>These authors contributed equally: Xintong Yao, Shanyue Sun. ✉e-mail: [quan.li@utsouthwestern.edu](mailto:quan.li@utsouthwestern.edu); [ying\\_yu@fudan.edu.cn](mailto:ying_yu@fudan.edu.cn); [zhengyuanting@fudan.edu.cn](mailto:zhengyuanting@fudan.edu.cn)

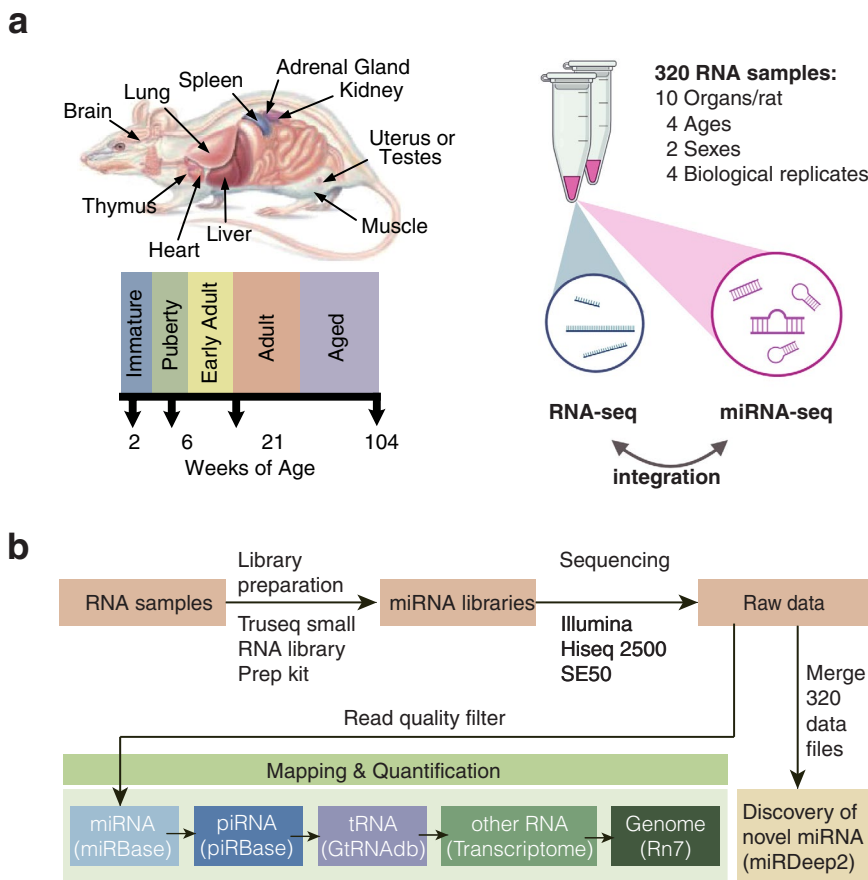


**Fig. 1** Overview of study design. 320 total RNA samples were collected from 16 female rats and 16 male rats of the Fisher 344 strain, including four rats for each sex under each of the four developmental stages, and ten organs (adrenal gland, brain, heart, kidney, liver, lung, muscle, spleen, thymus, testis, or uterus) per rat. Aliquots of the same RNA samples have also been used to construct mRNA dataset previously<sup>24,25</sup> (a), which makes it possible to integrate miRNA data with mRNA data. (b) Schematic overview of the miRNA-seq workflow: miRNA libraries were prepared and sequenced for each of the 320 samples. For miRNA quantification, adapter sequences were removed, followed by a read-quality filter. Reads of high quality were then mapped to miRBase, piRBase, GtRNADB, and the NCBI rat transcriptome and genome. In addition, reads from all 320 samples were pooled for novel miRNA discovery.

database consisting of miRNA-seq expression data across 14 organs among 12/13-week-old Sprague Dawley rats of both sexes<sup>17</sup>, through six sequencing batches. These studies mainly focused on miRNA expression differences among various organs. However, the diversity and number of expressed miRNAs in animals is not only organ-specific<sup>18,19</sup>, but also shows age dependence<sup>1,20,21</sup> and sex biases<sup>22,23</sup>. Specifically, the role of miRNAs in the aging process has often been overlooked and is therefore largely unclear.

Ideally, studies on rat transcriptome should simultaneously cover multiple organs across different developmental stages for both sexes. Indeed, in a widely cited previous study<sup>24,25</sup> as part of the Sequencing Quality Control (SEQC) consortium<sup>26</sup>, we constructed a comprehensive rat transcriptomic BodyMap with RNA-seq of 320 samples from 11 organs of both sexes of juvenile, adolescence, adult, and aged Fischer 344 rats and identified a large number of transcripts showing organ-specific, age-dependent, or sex-specific expression patterns. The unique rat mRNA dataset has already been widely used by scientific communities to advance our understanding of the dynamics of rat transcriptome, including studies on circRNAs<sup>27–29</sup>, the development of annotation tools<sup>30,31</sup>, and enrichment of database resources<sup>32,33</sup>.

Here, as a follow-up and complementary study, we constructed a comprehensive rat miRNA BodyMap by generating miRNA-seq data from the same 320 samples and described the quality and the dynamic characteristics of miRNA expression profiles across 11 organs, between two sexes, and over the life span of the rats (Fig. 1). We quantified 604 out of the 764 miRNAs annotated in miRbase v22.1 (<http://www.mirbase.org/>). In addition, to explore the potential of novel miRNA discovery with this dataset, we used the miRDeep2 algorithm<sup>34,35</sup> and identified 12 organ-enriched novel miRNA candidates. The miRNA-seq expression data were then analyzed in conjunction with the corresponding mRNA expression profiles. The quality of the miRNA-seq data was found to be high as seen from various aspects such as raw sequences, mapped sequences, and biological replicates.

The dataset we present here can help researchers study the characteristics of rat transcriptome and identify novel miRNAs. In addition, along with the mRNA dataset from the same set of samples, this miRNA-seq dataset provides a unique resource for data integration.

Name	Sequence
3'adapter	5'TGGAATTCTCGGGTGCAGG
5'adapter	5'GUUCAGAGUUCUACAGUCGCAGAUC
PCR primer (RP1)	5'AATGATACGGCACCACCGAGATCTACACGTTAGAGTTCTACAGTCCGA
PCR index primer	5' CAAGCAGAACGGCATACGAGAT[6 bases] GTGACTGGAGTTCCCTGGCACCCGAGAATTCCA

**Table 1.** Sequence information of the Truseq-small RNA kit.

## Methods

**Organ collection and RNA isolation.** Female and male Fischer 344 rats (pair-housed under standard conditions) from the National Center for Toxicological Research of the US Food and Drug Administration animal-breeding colony were euthanized by carbon dioxide asphyxiation at 2, 6, 21 and 104 week-of-age as previously described<sup>24,25</sup>. In summary, 320 tissue samples were derived from 16 female and 16 male rats of the Fischer 344 strain, including four rats for each sex under each of the four developmental stages and ten organs (adrenal gland, brain, heart, kidney, liver, lung, muscle, spleen, thymus, and testis or uterus) per rat. That is, four biological replicates per sample group were used in this study. Ground organ tissue was stored at  $-80^{\circ}\text{C}$ . Total RNA was extracted from ground tissue by using the miRNeasy Mini Kit (Qiagen) according to the manufacturer's protocol, including treatment with DNase. RNAs longer than 18 nucleotides were recovered with this method. The quality of each RNA sample was examined with an Agilent 2100 Bioanalyzer.

**Construction and sequencing of miRNA-seq libraries.** Small RNA libraries were constructed using Illumina TruSeq Small RNA Library Prep kit (the sequences of adapters and primers are provided in Table 1) by following the manufacturer's Reference Guide with some modifications. In brief, 1  $\mu\text{g}$  of total RNA (including miRNA) as input was sequentially ligated with 3' and 5' adapters, and the ligated RNA fragments were then reverse transcribed to single-stranded cDNAs using Superscript II reverse transcriptase (Invitrogen) and RT primer. The cDNAs were amplified by PCR with 13 cycles, and the resulting products were further purified with 2  $\times$  Agencourt AMPure XP beads (Beckman), followed by size selection using the Pippin Prep Size Selection System (Sage Science). The final libraries were validated using Agilent High Sensitivity DNA assay, and subjected to 50 bp single-end sequencing (SE50) on an Illumina HiSeq 2500. No spike-in controls or negative controls were used in the construction of this dataset.

**Pre-processing and processing of the reads.** The adapter sequences were removed with fastp 0.23.2 software (<http://opengene.org/fastp/fastp.0.23.2>), followed by a quality filter and a length filter. Reads with more than 2 "N" bases were discarded. The clipped reads with length between 16 and 35 nt were retained for alignment to various transcript types, including miRNA (miRbase v22.1, <http://www.mirbase.org/>), piRNA (piRBase, <http://www.regulatoryrna.org/database/piRNA/download.html>), tRNA (GtRNAdb, <http://gtrnadb.ucsc.edu/GtRNAdb2/genomes/eukaryota/Rnorv7/Rnorv7-seq.html>), other RNA (NCBI transcriptome, <https://www.ncbi.nlm.nih.gov/genome/73>), and the rat genome (Rn7, <https://hgdownload.soe.ucsc.edu/downloads.html#mammals>). The alignment was performed with Bowtie 1.3.1 (<http://bowtie-bio.sourceforge.net/manual.shtml>) with less than 2 mismatched bases allowed.

**Filtering of miRNAs and samples.** The following strategies were used to filter miRNAs and samples of questionable quality: (1) the low-expressed miRNAs less than one count per library on average, were discarded. (2) a sample was removed if it failed to cluster with other samples from the same organ type in a hierarchical clustering analysis. Spl\_F\_104\_4 and Brn\_M\_006\_3 samples were removed, as they clustered to uterus samples instead of spleen and brain, respectively. Ultimately, a miRNA expression matrix with 604 miRNAs and 318 samples was obtained for further analysis.

**Identification of novel miRNA candidates.** First, reads from all 320 samples were pooled for identification of novel miRNA candidates. Using the mapper module provided within miRDeep2.0.1.3, raw reads of the merged samples were subjected to a series of stringent filters (discarding low-quality reads and reads with fewer than 18 nt after clipping the 3' adapter), and the remaining sequences were then mapped to the rat genome reference (Rn7). Next, the mapped reads were submitted to the miRDeep2 module to detect novel miRNAs with default parameters. Novel miRNAs that have passed the stringent filters (miRDeep2 score  $\geq 10$ , significant Ranfold  $P$ -value and no rfam alert of the possibility of being a rRNA) were selected as the potential novel miRNA candidates.

To validate the organ-specificity of the novel miRNA candidates, we quantified the novel miRNA expressions across 320 samples and performed differential expression analysis between any two organs at each developmental stage. A miRNA is considered 'organ-specific' if it is over-expressed by at least 1.5 fold (fold-change  $> 1.5$  and adjusted  $P$ -value  $< 0.05$ ) in one organ over all other organs and across all four developmental stages. Finally, the 12 organ-specific sequences were reported as novel miRNA candidates in Online-only Table 1.

## Data Records

The miRNA-seq dataset generated in study is available in the NCBI Gene Expression Omnibus (GEO) with series accession number GSE172269<sup>36</sup>. This accession contains both the raw sequence data files (fq.gz format) and the processed data files (raw counts of mapped sequencing reads) used in this report. All data can be used without restrictions.

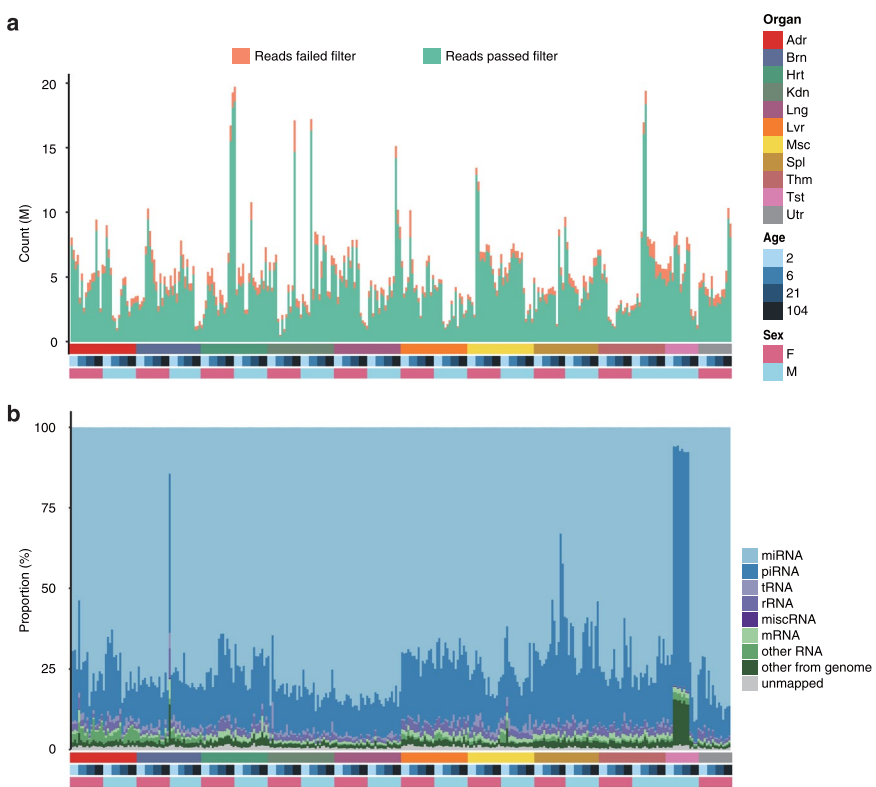


**Fig. 2** Quality of sequencing reads. **(a)** The overall height of each bar represents the number of total reads sequenced from each RNA sample, and the green part and orange part correspond to the reads which either passed or failed the quality filter, respectively. High-quality reads entered the following mapping workflow. **(b)** Percentages of the reads that mapped to miRNA, piRNA, tRNA, rRNA, miscRNA, mRNA, other RNA, as well as the reads that mapped to none of the aforementioned transcript types but mapped to the rat genome, are represented by different colours. Abbreviation for organs, Adr, adrenal; Brn, brain; Hrt, heart; Kdn, kidney; Lng, lung; Lvr, liver; Msc, skeletal muscle; Spl, spleen; Thm, thymus; Tst, testis; and Utr, uterus.

### Technical Validation

**Quality of RNA samples.** The quality of RNA samples was assessed with an Agilent Bioanalyzer. Most samples showed good RNA Integrity Number (RIN  $9.08 \pm 1.08$ , mean  $\pm$  sd), except for the eight week-2 spleen samples with RIN below 5.2. The RNA integrity numbers of all the 320 samples were listed in Online-only Table 2.

**Quality of libraries.** The quality of miRNA sequencing data for each sample was checked (Fig. 2). Briefly, a total of 1.6 billion raw reads was obtained, with 5.1 million reads per sample on average, which is sufficient for miRNA quantification. After quality filtering and length filtering,  $4.5 \pm 2.8$  million reads of high quality were retained per sample on average (Fig. 2a). The proportions of various transcript types of these reads were demonstrated in Fig. 2b. The majority of libraries were contributed by miRNA and piRNA sequences, followed by tRNA, rRNA, mRNA and other sequences from the rat transcriptome and genome. Most libraries were dominated by miRNA reads ( $75.6 \pm 8.5\%$ ), except for the testis samples from the adolescent and adult rats, which were dominated by piRNA ( $73.8 \pm 0.8\%$ ). However, the proportion of miRNA for the Brn\_F\_104\_4 sample was 14.4%, much lower than the average proportion of brain samples.

**Reproducibility of biological replicates.** To assess the reproducibility of biological replicates, we calculated the Pearson's correlation coefficients between any two of the 320 samples (Fig. 3a–c). The Pearson's correlation coefficients between miRNA expressions of biological replicates from the same group ( $0.98 \pm 0.01$ , mean  $\pm$  sd) were much higher than those from different sample groups ( $0.82 \pm 0.09$ ) (Fig. 3a). This result indicated good consistency among biological replicates in which biological variations between animals and technical variations between sample processing were included. Moreover, this conclusion was further confirmed in principal component analysis, from which the majority of biological replicates could be grouped together (Fig. 4a–d).

**Validation of organ specific signature.** To obtain an overview of miRNA expression profiles, we performed principal component analysis and hierarchical clustering (Fig. 4a–e). The miRNA profiles were discriminating among different organs (Fig. 4e). To identify the miRNAs that contribute the most to organ-specific expression, we set out to identify 'organ-enriched' miRNAs. A miRNA is considered 'organ-enriched' if it is over-expressed by at least four folds in one organ over any other organs and across all four developmental stages, a quite stringent criterion. Consequently, 67 organ-enriched miRNAs were identified, including a novel miRNA candidate. The z-scaled expression levels of these miRNAs were shown in Fig. 5a.

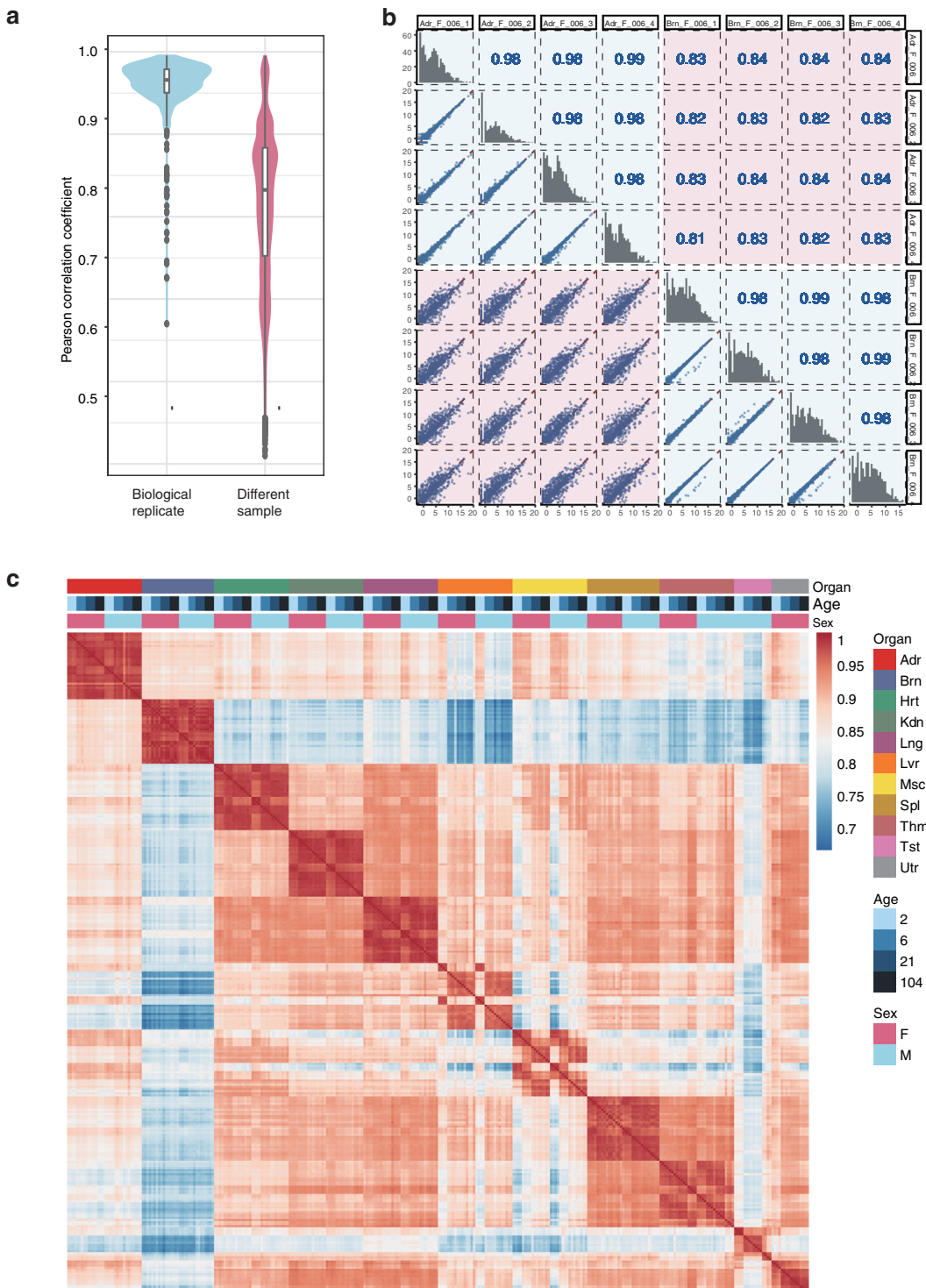


**Fig. 3** Reproducibility of biological replicates. **(a)** Distributions of the pairwise Pearson correlation coefficients between the biological replicates (navy blue) and between samples from different groups (light blue). **(b)** Correlations between four biological replicates from each of two particular groups (adrenal gland and brain samples of female rats at week 6) were demonstrated as an example. **(c)** Pairwise Pearson correlation coefficients between miRNA expressions of the 318 samples. Abbreviation for organs, Adr, adrenal; Brn, brain; Hrt, heart; Kdn, kidney; Lng, lung; Lvr, liver; Msc, skeletal muscle; Spl, spleen; Thm, thymus; Tst, testis; and Utr, uterus.

To independently validate the organ-enriched miRNAs discovered in this study, the literature-reported miRNA profiles of 55 different organs and tissues from normal male rats based on Agilent miRNA microarrays were used<sup>15</sup>. Thirty-one (31) organ-enriched miRNAs identified in our study, including brain-enriched, testis-enriched, liver-enriched, and spleen-enriched and heart-enriched miRNAs, were also profiled in the

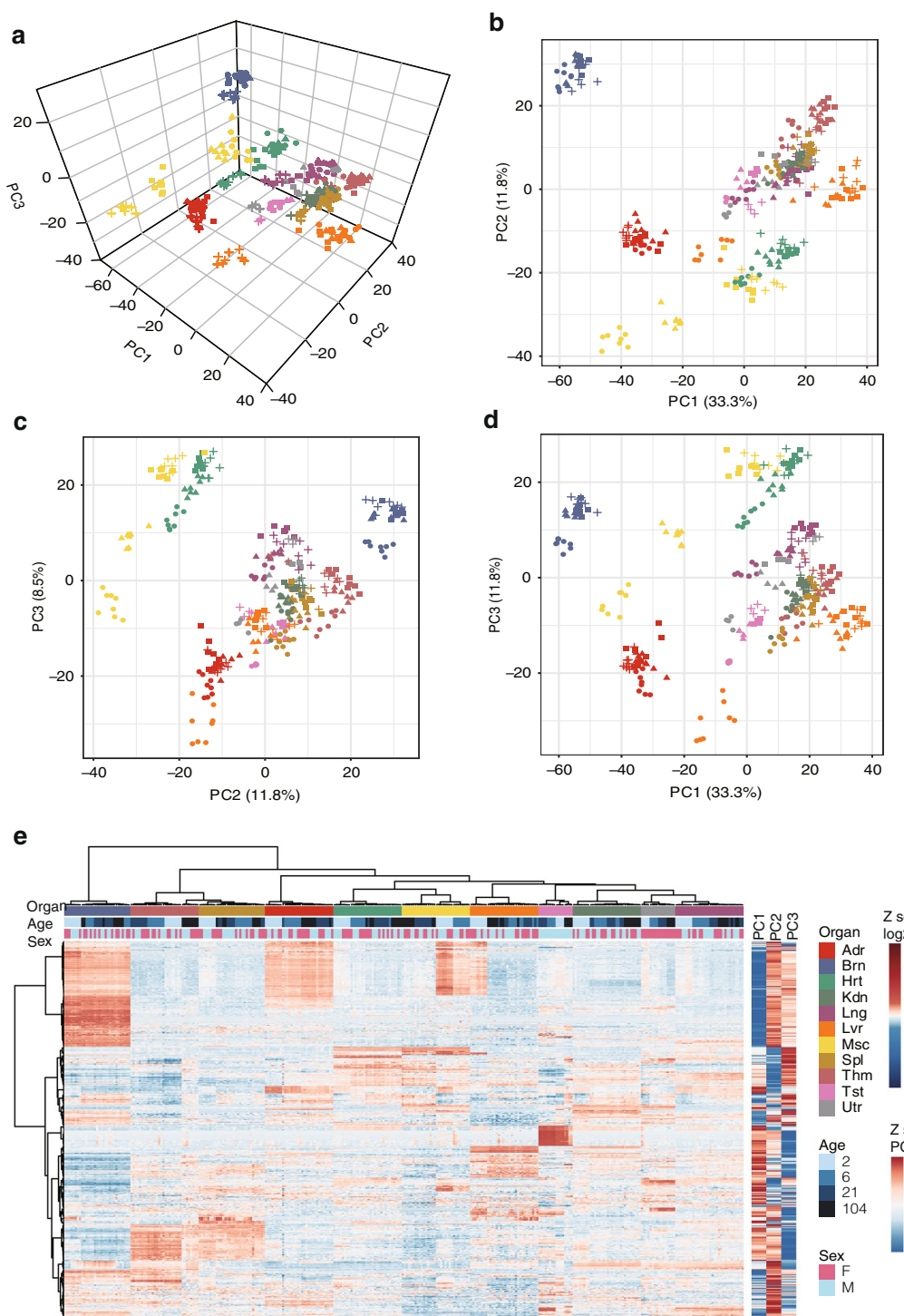


**Fig. 4** Expression profiles of miRNAs are discriminating among different organs. miRNA expression profiles are depicted by the top three principal components (**a–d**). Each point corresponds to one of the 318 samples. Samples from different organs are represented by different colours, and those of different ages are represented by different shapes. (**e**) Hierarchical clustering analysis (HCA) of expression profiles from 318 rat samples with 604 miRNAs. Heatmap (left) for normalized log<sub>2</sub> (CPM) values. Right, normalized loadings of each miRNA for the top three PCs. Abbreviation for organs, Adr, adrenal; Brn, brain; Hrt, heart; Kdn, kidney; Lng, lung; Lvr, liver; Msc, skeletal muscle; Spl, spleen; Thm, thymus; Tst, testis; and Utr, uterus.

miRNA microarray dataset and displayed a pattern of high-level expression in biological systems with functions similar to those of the organs examined in this study (Fig. 5b). This result confirmed the reliability of the organ specific signature presented in our dataset.

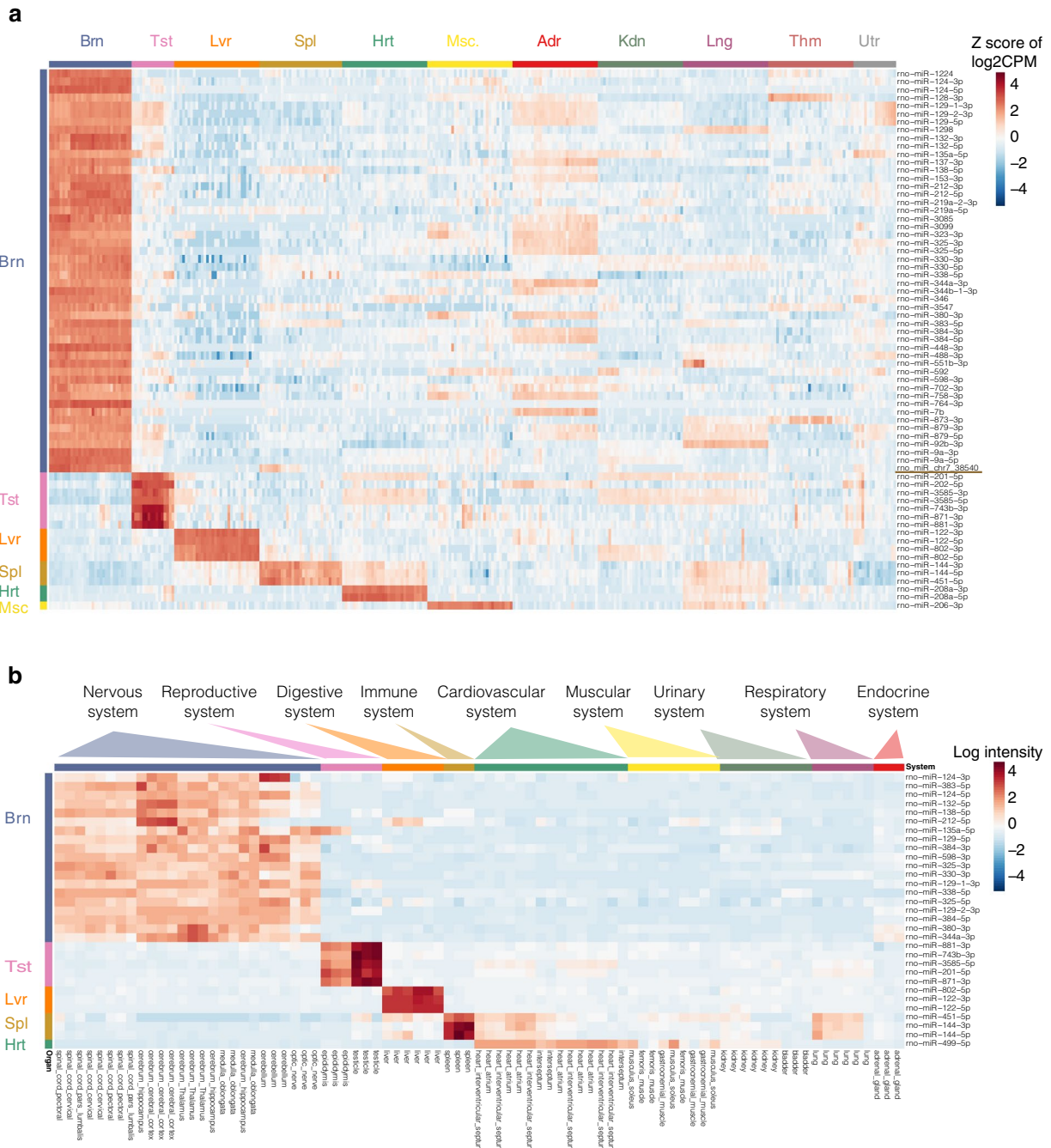


**Fig. 5** Validation of organ-specific miRNA signatures in a microarray dataset. **(a)** Expression profiles of 67 organ-enriched miRNAs across 318 samples are arranged by organ type. Expression data were Z-score scaled per gene across all 318 samples. Each row represents a miRNA that is enriched in an organ. **(b)** Expression profiles of 31 organ-enriched miRNAs across 23 tissues in the microarray miRNA expression dataset of Minami *et al.*<sup>15</sup> are arranged by biological system. Each row represents a miRNA that is enriched in an organ. Each column represents a sample profiled in the microarray dataset. Abbreviation for organs, Adr, adrenal; Brn, brain; Hrt, heart; Kdn, kidney; Lng, lung; Lvr, liver; Msc, skeletal muscle; Spl, spleen; Thm, thymus; Tst, testis; and Utr, uterus.

**Reliability of miRNA-mRNA integration.** To examine the reliability of miRNA-mRNA integration using the miRNA dataset presented here and the previously published mRNA dataset, we compared the source of variability in these two datasets. Principal variance component analysis was performed on miRNA and mRNA expression profiles respectively (Fig. 6a). As expected, the ‘organ’ factor accounted for the most total variance in both datasets, with 61.6% for miRNA and 64.2% for mRNA profiles. The variance attributable to each factor was similar in the mRNA and miRNA datasets, except for age. The overall expression difference due to age was significantly higher for miRNA (11.7%) than that for mRNA (1.7%) expression. However, there was a stronger interaction between age and organ type for miRNA (15.7%) compared to that for mRNA (2.5%) expression. It

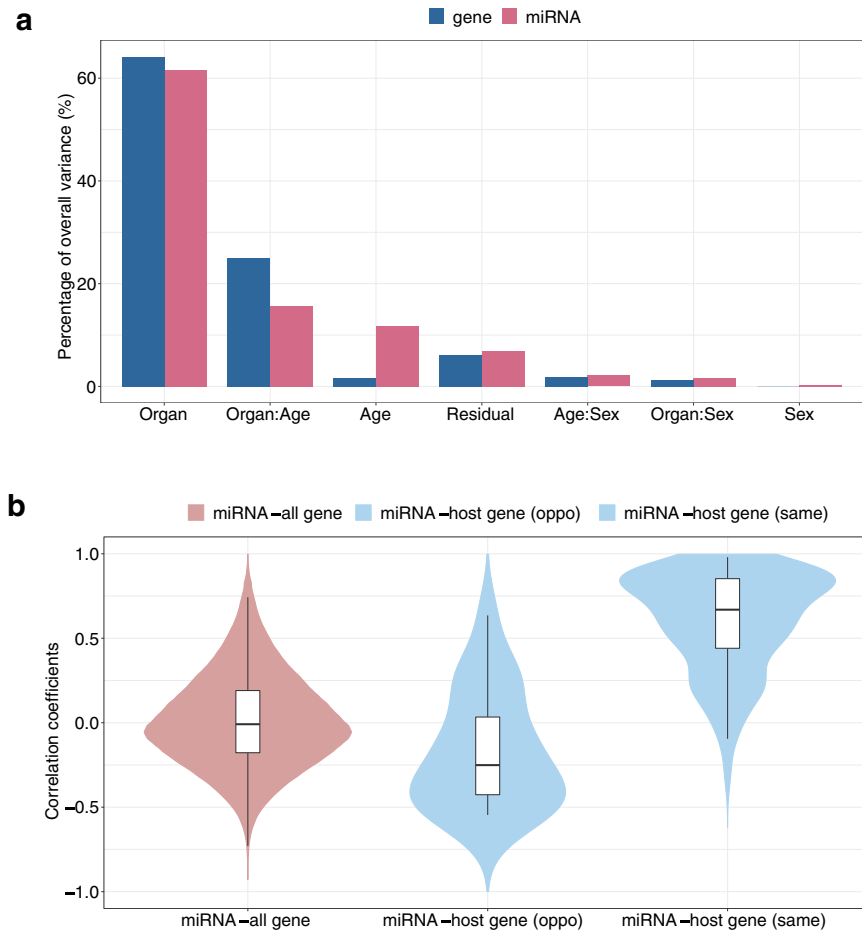


**Fig. 6** Reliability of miRNA-mRNA integration. **(a)** Principal variance component analysis (PVCA) shows the relative contribution of main effects (organ, age, sex, and replicate) and interactions (:) to total model variance in miRNA (blue) and gene (red) expression. Effects in the Y-axis are ordered by proportion of overall variations explained in the miRNA dataset. **(b)** Pairwise correlations between all 10,418,396 miRNA-gene pairs (604 miRNAs versus 17,249 genes), 20 intragenic miRNAs on opposite strand of host genes, 147 intragenic miRNAs on the same strand of host genes.

appeared that there is a more dynamic miRNA expression pattern across the four developmental stages independent of organ types, whereas the temporal expression of mRNA appeared to be more organ dependent than that of miRNA expression. These results highlight the concordance of the two datasets.

Meanwhile, the genomic locus of miRNA genes was used to test the reliability of the association between these miRNA and mRNA datasets. We calculated the correlations between expression levels of miRNAs and those of genes (miRNA-gene pairs). The distributions of correlations between several types of miRNA-gene pairs were demonstrated in Fig. 6b. The correlations between all miRNA-gene pairs were weak ( $0.01 \pm 0.28$ , median  $\pm$  sd) as expected. Importantly, the co-transcription events of miRNA and host genes were observed in these datasets, as the expressions of intragenic miRNAs were highly positively correlated with those of their host genes on the same strand ( $0.60 \pm 0.29$ , N = 179). In addition, the slightly negative correlations ( $-0.17 \pm 0.35$ ) between these miRNAs-host genes (opp) pairs confirmed that co-expression events are rare when intragenic miRNAs and the host genes are located on the opposite strands. In summary, the miRNA dataset along with the mRNA datasets provided a reliable and unique resource for integration.

### Code availability

The code required for reproducing the figures and tables is freely available on GitHub (<https://github.com/XintongYao-96/Rat-microRNA-Bodymap>).

Received: 20 May 2021; Accepted: 4 March 2022;

Published online: 12 May 2022

### References

1. Sun, K. & Lai, E. C. Adult-specific functions of animal microRNAs. *Nat Rev Genet* **14**, 535–548, <https://doi.org/10.1038/nrg3471> (2013).
2. Shukla, G. C., Singh, J. & Barik, S. MicroRNAs: Processing, Maturation, Target Recognition and Regulatory Functions. *Mol Cell Pharmacol* **3**, 83–92 (2011).

3. Bartel, D. P. MicroRNAs: target recognition and regulatory functions. *Cell* **136**, 215–233, <https://doi.org/10.1016/j.cell.2009.01.002> (2009).
4. Ambros, V. The functions of animal microRNAs. *Nature* **431**, 350–355 (2004).
5. Lai, E. C. Micro RNAs are complementary to 3' UTR sequence motifs that mediate negative post-transcriptional regulation. *Nat Genet* **30**, 363–364, <https://doi.org/10.1038/ng865> (2002).
6. Goodall, G. J. & Wickramasinghe, V. O. RNA in cancer. *Nat Rev Cancer* **21**, 22–36, <https://doi.org/10.1038/s41568-020-00306-0> (2021).
7. Berindan-Neagoe, I., Monroe Pdel, C., Pasculle, B. & Calin, G. A. MicroRNAome genome: a treasure for cancer diagnosis and therapy. *CA Cancer J Clin* **64**, 311–336, <https://doi.org/10.3322/caac.21244> (2014).
8. Pratama, M. Y., Visintin, A., Croce, L. S., Tiribelli, C. & Pascut, D. Circulatory miRNA as a Biomarker for Therapy Response and Disease-Free Survival in Hepatocellular Carcinoma. *Cancers (Basel)* **12**, <https://doi.org/10.3390/cancers12102810> (2020).
9. Wang, X., He, Y., Mackowiak, B. & Gao, B. MicroRNAs as regulators, biomarkers and therapeutic targets in liver diseases. *Gut* **70**, 784–795, <https://doi.org/10.1136/gutjnl-2020-322526> (2021).
10. Liu, A. et al. Antagonizing miR-455-3p inhibits chemoresistance and aggressiveness in esophageal squamous cell carcinoma. *Mol Cancer* **16**, 106, <https://doi.org/10.1186/s12943-017-0669-9> (2017).
11. Vira, D. et al. Cancer stem cells, microRNAs, and therapeutic strategies including natural products. *Cancer Metastasis Rev* **31**, 733–751, <https://doi.org/10.1007/s10555-012-9382-8> (2012).
12. Hayes, J., Peruzzi, P. P. & Lawler, S. MicroRNAs in cancer: biomarkers, functions and therapy. *Trends Mol Med* **20**, 460–469, <https://doi.org/10.1016/j.molmed.2014.06.005> (2014).
13. Kozomara, A. & Griffiths-Jones, S. miRBase: annotating high confidence microRNAs using deep sequencing data. *Nucleic Acids Res* **42**, D68–73, <https://doi.org/10.1093/nar/gkt1181> (2014).
14. Kozomara, A., Birgaoanu, M. & Griffiths-Jones, S. miRBase: from microRNA sequences to function. *Nucleic Acids Res* **47**, D155–D162, <https://doi.org/10.1093/nar/gky1141> (2019).
15. Minami, K. et al. miRNA expression atlas in male rat. *Sci Data* **1**, 140005, <https://doi.org/10.1038/sdata.2014.5> (2014).
16. Bushel, P. R. et al. RATEmiRs: the rat atlas of tissue-specific and enriched miRNAs database. *Bmc Genomics* **19**, 825, <https://doi.org/10.1186/s12864-018-5220-x> (2018).
17. Smith, A. et al. The Rat microRNA body atlas; Evaluation of the microRNA content of rat organs through deep sequencing and characterization of pancreas enriched miRNAs as biomarkers of pancreatic toxicity in the rat and dog. *Bmc Genomics* **17**, 694, <https://doi.org/10.1186/s12864-016-2956-z> (2016).
18. Sun, Y. et al. Development of a micro-array to detect human and mouse microRNAs and characterization of expression in human organs. *Nucleic Acids Res* **32**, e188, <https://doi.org/10.1093/nar/gnh186> (2004).
19. Smibert, P. et al. Global patterns of tissue-specific alternative polyadenylation in Drosophila. *Cell Rep* **1**, 277–289, <https://doi.org/10.1016/j.celrep.2012.01.001> (2012).
20. Baloun, J. et al. Epilepsy miRNA Profile Depends on the Age of Onset in Humans and Rats. *Front Neurosci* **14**, 924, <https://doi.org/10.3389/fnins.2020.00924> (2020).
21. Meder, B. et al. Influence of the confounding factors age and sex on microRNA profiles from peripheral blood. *Clin Chem* **60**, 1200–1208, <https://doi.org/10.1373/clinchem.2014.224238> (2014).
22. Veltsos, P., Fang, Y., Cossins, A. R., Snook, R. R. & Ritchie, M. G. Mating system manipulation and the evolution of sex-biased gene expression in Drosophila. *Nat Commun* **8**, 2072, <https://doi.org/10.1038/s41467-017-02232-6> (2017).
23. Cui, C. et al. Identification and Analysis of Human Sex-biased MicroRNAs. *Genomics Proteomics Bioinformatics* **16**, 200–211, <https://doi.org/10.1016/j.gpb.2018.03.004> (2018).
24. Yu, Y. et al. A rat RNA-Seq transcriptomic BodyMap across 11 organs and 4 developmental stages. *Nat Commun* **5**, 3230, <https://doi.org/10.1038/ncomms4230> (2014).
25. Yu, Y. et al. Comprehensive RNA-Seq transcriptomic profiling across 11 organs, 4 ages, and 2 sexes of Fischer 344 rats. *Sci Data* **1**, 140013, <https://doi.org/10.1038/sdata.2014.13> (2014).
26. Su, Z. et al. A comprehensive assessment of RNA-seq accuracy, reproducibility and information content by the Sequencing Quality Control Consortium. *Nat. Biotechnol.* **32**, 903–914, <https://doi.org/10.1038/nbt.2957> (2014).
27. Gong, B., Xu, J. & Tong, W. Landscape of circRNAs Across 11 Organs and 4 Ages in Fischer 344 Rats. *Chem Res Toxicol* <https://doi.org/10.1021/acs.chemrestox.0c00144> (2020).
28. Zhou, T. et al. Rat BodyMap transcriptomes reveal unique circular RNA features across tissue types and developmental stages. *RNA* **24**, 1443–1456, <https://doi.org/10.1261/rna.067132.118> (2018).
29. You, X. et al. Neural circular RNAs are derived from synaptic genes and regulated by development and plasticity. *Nat Neurosci* **18**, 603–610, <https://doi.org/10.1038/nn.3975> (2015).
30. Ji, X. et al. A comprehensive rat transcriptome built from large scale RNA-seq-based annotation. *Nucleic Acids Res* **48**, 8320–8331, <https://doi.org/10.1093/nar/gkaa638> (2020).
31. Wen, Z. et al. Expression profiling and functional annotation of noncoding genes across 11 distinct organs in rat development. *Sci Rep* **6**, 38575, <https://doi.org/10.1038/srep38575> (2016).
32. Palasca, O., Santos, A., Stolte, C., Gorodkin, J. & Jensen, L. J. TISSUES 2.0: an integrative web resource on mammalian tissue expression. *Database (Oxford)* **2018**, <https://doi.org/10.1093/database/bay028> (2018).
33. Wang, J. et al. MARRVEL: Integration of Human and Model Organism Genetic Resources to Facilitate Functional Annotation of the Human Genome. *Am. J. Hum. Genet.* **100**, 843–853, <https://doi.org/10.1016/j.ajhg.2017.04.010> (2017).
34. Friedlander, M. R., Mackowiak, S. D., Li, N., Chen, W. & Rajewsky, N. miRDeep2 accurately identifies known and hundreds of novel microRNA genes in seven animal clades. *Nucleic Acids Res* **40**, 37–52, <https://doi.org/10.1093/nar/gkr688> (2012).
35. Friedlander, M. R. et al. Discovering microRNAs from deep sequencing data using miRDeep. *Nat Biotechnol* **26**, 407–415, <https://doi.org/10.1038/nbt1394> (2008).
36. Gene Expression Omnibus <https://identifiers.org/geo:GSE172269> (2021).

## Acknowledgements

RNA samples for miRNA sequencing were leftovers from an early study for RNA sequencing (Yu Y et al., *Nature Communications* and *Scientific Data* 2014) and were originally obtained by Dr. James C. Fusco's laboratory at the National Center for Toxicological Research of the US Food and Drug Administration, Jefferson, AR, USA. This study was supported in part by the National Key R&D Program of China (2018YFE0201603), the National Natural Science Foundation of China (32170657), and Shanghai Municipal Science and Technology Major Project (2017SHZDZX01). Figure 1 was created with Biorender.com.

## Author contributions

Y.T.Z. and Q.L. conceived the research. miRNA-seq libraries were constructed by G.C. and Q.L. Sequencing data acquisition, data management and scientific support was performed and overseen by J.Y., Y.T.Z., Y.Y. and L.S. Data analysis and interpretation were performed by X.Y., S.S., Y.Z., Y.L., J.Y., L.R., Z.C., W.H., Y.S., J.S., H.J., Z.L., H.W., P.Z., L.S., Q.L., Y.Y. and Y.T.Z. The manuscript was written and revised by X.Y., S.S., Y.T.Z., Y.Y., Q.L. and L.S. All authors reviewed and approved the submitted manuscript.

## Competing interests

The authors declare no competing interests.

## Additional information

**Correspondence** and requests for materials should be addressed to Q.-Z.L., Y.Y. or Y.Z.

**Reprints and permissions information** is available at [www.nature.com/reprints](http://www.nature.com/reprints).

**Publisher's note** Springer Nature remains neutral with regard to jurisdictional claims in published maps and institutional affiliations.



**Open Access** This article is licensed under a Creative Commons Attribution 4.0 International License, which permits use, sharing, adaptation, distribution and reproduction in any medium or format, as long as you give appropriate credit to the original author(s) and the source, provide a link to the Creative Commons license, and indicate if changes were made. The images or other third party material in this article are included in the article's Creative Commons license, unless indicated otherwise in a credit line to the material. If material is not included in the article's Creative Commons license and your intended use is not permitted by statutory regulation or exceeds the permitted use, you will need to obtain permission directly from the copyright holder. To view a copy of this license, visit <http://creativecommons.org/licenses/by/4.0/>.

© The Author(s) 2022